Research Square

Preprints are preliminary reports that have not undergone peer review.
They should not be considered conclusive, used to inform clinical practice,
or referenced by the media as validated information.

# Performance of the DLPNO-CCSD and Recent DFT Methods in the Calculation of Isotropic and Dipolar Contributions to 14N Hyperfine Coupling Constants of Nitroxide Radicals

**Oleg Gromov** ( aalchm@gmail.com )
Moskovskij gosudarstvennyj universitet imeni M V Lomonosova Himiceskij fakul'tet https://orcid.org/0000-0002-4119-8602

**Research Article**

**Keywords:** EPR spectroscopy, nitroxide radical, DFT, hyperfine coupling, DLPNO-CCSD

**Posted Date:** March 11th, 2021

**DOI:** https://doi.org/10.21203/rs.3.rs-279592/v1

**License:** This work is licensed under a Creative Commons Attribution 4.0 International License. Read Full License

## Abstract

In the present study, the performance of a set of density functionals: BP86, PBE, OLYP, BEEF, PBEpow, TPSS, SCAN, PBEGXPBE, M06L, MN15L, B3LYP, PBE0, mPW1PW, B97, BHandHLYP, mPW1PW, HSE06, B98, TPSS0, PBE1KCIS, SCAN0, M06, M06-2X, MN15, CAM-B3LYP, ωB97x, B2PLYP, and the B3LYP/N07D and PBE/N07D schemes in the calculation of the $^{14}$N anisotropic hyperfine coupling (HFC) constants of a set of 23 nitroxide radicals is evaluated. The results are compared with those obtained with the DLPNO-CCSD method and experimental HFC values. Harmonic contribution to the $^{14}$N HFC vibrational correction was calculated at the revPBE0/def2-TZVPP level and included in the evaluation. With the vibrational correction, the DLPNO-CCSD method yielded HFC values in good agreement with the experiment (MAD = 0.3 G for the dipole-dipole contribution and MAD = 0.8 G for the contact coupling contribution). The best DFT results are obtained using the M06 functional with mean absolute deviation (MAD) = 0.2 G for the dipole-dipole contribution and MAD = 0.7 G for the contact coupling contribution. In general, vibrational correction significantly improved most DFT functionals' performance but did not change its overall ranking.


## Introduction

Density functional theory (DFT) is now the most used method in quantum chemical modeling as it affords the best balance of cost and accuracy for the time being. Though DFT itself is an exact theory connecting the molecular system's many-electron density with its energy via “exact” density functional, it relies on approximate functionals in practical applications. Hence many general-purpose and particular property tailored functionals were developed for the last few decades [1]. New functionals are supposed to perform better than the older ones. However, the common practice shows that one should not always prefer some newly developed techniques over the previous ones thoughtlessly. Indeed as shown in the paper by Medvedev et al. [2], the common strategy of DFT functional development tailoring molecular energetics and geometry might result in DFT functionals poorly describing electron density. While energy-based evaluation of DFT functionals’ performance readily delivers natural metrics, electron density-based evaluation metrics are more ambiguous; see for discussion Marjewski et al. [3] and the references therein. Though electron density also delivers some natural and experimentally observable metrics such as (deviation in calculated) dipole moment (and higher moments) as used by Hait and Head-Gordon [4]. Interestingly Hait and Head-Gordon found open-shell species to be the most difficult cases for DFT. Some open-shell species, namely radicals (including some coordination compounds), deliver another electron density-based natural metric: hyperfine coupling (HFC) [5]. One can extract some information on spin density distribution in the radical from HFC directly measured by Electron Paramagnetic Resonance (EPR) spectroscopy and use it in DFT functionals performance evaluation [5–7].

EPR spectroscopy is a widely used method in studying organic radicals and d-block metal complexes [8]. To interpret experimental EPR spectra, one usually uses an effective spin Hamiltonian describing the interaction between an electron spin ($\hat{\boldsymbol{S}}$), magnetic nuclei spins ($\hat{\boldsymbol{I}}$), and an external magnetic field ($\boldsymbol{B}$): **see formula 1 in the supplementary files.**

The first term is the Zeeman interaction between the electron spin and the external magnetic field, with $\boldsymbol{g}$ being a 3x3 tensor. The hyperfine coupling tensors $\boldsymbol{A}_i$ describe the interaction of the unpaired electron and the magnetic moments of the nuclei $\hat{\boldsymbol{I}}_i$. The hyperfine coupling tensor can be divided into the isotropic ($a_{iso}$) and the traceless spin-dipole contributions: **see formula 2 in the supplementary files.**

where the isotropic Fermi contact term **see formula 3 in the supplementary files.**

readily delivers the spin density at the nucleus N ($\rho(\mathbf{R}_N)$ ), while $\boldsymbol{A}^{dip}$ tensor depends on the whole spin density distribution.

In the previous paper [6], we evaluated the well-established and widely used functionals. During the last decade, many new functionals arrived. For example, the strongly constrained and appropriately normed semilocal density functional (SCAN) yields at the cost of a non-hybrid mGGA functional [2] electron densities better than the B3LYP functional. While the B3LYP functional is well tested [5, 7, 9–14], the SCAN functional performance data are insufficient. It has been shown [5, 15] that SCAN, while being competitive to the commonly used functionals in some cases, is not, in general, the best choice for HFC calculation. In some cases, SCAN and SCAN0 functionals even predicted qualitatively incorrect electronic structures of transition metal complexes [15]. For that reason, it is interesting to expand this research on the SCAN performance on compounds of p-elements. The B98, PBE1KCIS, HSE06, and SCAN functionals are listed in the paper by Medvedev et al. among the best functionals for electron density and are included in the present research.

The DFT calculations results can be compared either with the experimental values or with the values calculated using some accurate *ab initio* method. The former requires taking into account solvation and vibrational averaging effects and calculating accurate geometry[16]. The latter way, which requires, for example, coupled-cluster calculation of the reference values, is therefore preferred, especially if the test set consists of small species, easily treated using accurate *ab initio* methods. Both choices of the reference are consistent. For example, the coupled cluster methods as shown by Barone and Puzzarini [16] for small $X_2NO$ Systems (X = F, Cl, Br, I), bring HFC constants in excellent agreement with the experiment, given vibrational, media, and basis set effects are taken into account in CCSD(T) calculation. A routine CCSD calculation of substantially large radical systems was recently made possible in the domain-based local pair-natural orbital coupled-cluster with singles and doubles (DLPNO-CCSD) framework [17]. Hence it is possible to use both references even for large radical systems. Besides, it is interesting to evaluate the DLPNO-CCSD method performance for "real-life" nitroxide radicals.

## Calculation Details

ORCA 4.2.0 program package [18] was used to perform all calculations. The nitroxide radicals' geometries were optimized at the UKS/B2GP-PLYP/def2-TZVPP [19, 20] level with the COSMO solvation model [21]. The B2GP-PLYP functional was chosen for geometry optimization according to a recent benchmark study [22].

$^{14}N$ HFCC were calculated using some newer density functionals available in Libxc [23]. DFT functionals used are: strongly constrained and appropriately normed semilocal density functional (SCAN) [24] (we didn't find significant differences between the results of SCAN and revised SCAN functional [25] hence the results of the calculations using the latter are not presented), hybrid SCAN0 [26] (also similar to the results of the revised version), bayesian error estimation functional (BEEF) [27], power series extension of the PBE exchange functional [28] (PBEpow exchange functional combined with the PBE [29] correlation functional), PBE-GX functional [30] (combined with the PBE correlation functional), MN15 and MN15-L functionals [31, 32], PBE1KCIS hybrid [33] (with KCIS correlation functional [34]), screened Coulomb potential hybrid functional (HSE06) [35] and B98 hybrid [36]. We compared these functionals with the functionals used in our previous paper [6]: GGA functionals BP86 [37, 38], PBE [29], OLYP [39]; the meta-GGA functionals TPSS [40], M06L [41]; the hybrid GGA functionals B3LYP [42], PBE0 [43], mPW1PW [44], B97 [45], BHandHLYP [46]; the hybrid meta-GGA functionals TPSS0 [40], M06 [47], M06-2X [47]; the range-separated functionals CAM-B3LYP [48], ωB97x [49], the double-hybrid functional B2PLYP (with relaxed density) [50]. The B3LYP/N07D and PBE0/N07D functional/basis combinations [51, 52] were also used. All DFT calculations were performed using unrestricted Kohn-Sham formalism.

Basis sets for coupled-cluster and DFT calculations were constructed similarly to the one used by Datta and Gauss [53]. DFT calculations were performed using uncontracted cc-pCVQZ basis set [54] augmented with four tight even-tempered s-functions (denoted cc-pCVQZ-Juc by analogy with an aug-cc-pVTZ-Juc basis set of Sauer et al. [55]). For further discussion on the basis sets for HFC calculations, see Jakobsen and Jensen [56]. The RIJCOSX [57] approximation with auto-generated auxiliary basis sets [58] and integration grid Grid7 (the tightest in ORCA) and Gridx9 were used throughout except for the calculation of the vibrational correction. In the case of dubious results, calculations were performed without RI or RIJCOSX approximations (for example, calculations using the MN15, SCAN, and SCAN0 functionals). The COSMO solvation model [21] with toluene as a solvent was used as non-polar solvents implicit solvation models were shown to yield reasonable solvent shifts [16, 59].

$^{14}N$ hyperfine couplings of nitroxide radicals were also calculated using the domain-based local pair-natural orbital coupled-cluster with singles and doubles (DLPNO-CCSD) method [17, 60, 61] with DLPNO-HFC1 set of the thresholds and quasi-restricted orbitals (QRO) from unrestricted B3LYP/COSMO calculation as a reference. COSMO could not be used in DLPNO-CCSD calculation directly. However, the introduction of solvation at the reference level yields results similar to those obtained using an additive scheme of Barone [16]. $T_1$ diagnostic parameter values were always lower than 0.02. DLPNO-CCSD calculations were performed using uncontracted cc-pCVTZ basis set [54] augmented with four tight s-functions from aug-cc-pVTZ-J [55] basis set.

Vibrational corrections to isotropic hyperfine coupling constants were calculated using the perturbative approach [62–66]. Only harmonic corrections, given by**: see formula 4 in the supplementary files.**

$^{14}N$ hyperfine coupling constants of 23 nitroxide radicals (Fig. 1) used as the reference were taken from Lebedev et al. [68]. The choice of particular radicals was discussed in our previous paper [6]. $^{14}N$ isotropic hyperfine coupling constants ($a_{iso}$) were calculated from

the hyperfine coupling tensors at low temperatures. The labels used for nitroxide radicals by Lebedev et al. were adopted for use in the present paper.

## Results And Discussion

### 3.1 DLPNO-CCSD calculation and ZPVC

The experimental data by Lebedev et al. [68] were acquired at low temperatures, and vibrational averaging effects are reduced to some extent. For example, Barone et al. [65] estimated ZPVC to $^{14}N$ $a_{iso}$ of the 2,2,5,5-tetramethylpyrrolidin-1-yl)oxydanyl radical (Proxyl, pyrrolidine series) to be 0.3 G at 0 K (harmonic contribution is 0.2 G and anharmonic contribution is 0.14 G). We omitted vibrational corrections in our previous [6] due to this relatively low value. On the other hand, Barone et al. [59] estimated vibrational correction to $^{14}N$ $a_{iso}$ of the Proxyl radical at 298 K to be up to 2.6 G. Recently Auer et al. calculated ZPVC of 2,2,3,4,5,5-hexamethylperhydroimidazol-1-oxyl radical (HMI, imidazolidine series) at the revPBE0 level (0.9 G) and the DLPNO-CCSD level (1.3G).

In the present study, $^{14}N$ HFCCs were calculated at the DLPNO-CCSD level (table 1). The relative error of the DLPNO-CCSD calculation to experiment varies from 7% up to 22%. Moreover, the correlation of calculated and experimental $^{14}N$ $a_{iso}$ (Fig. 4, black) is not linear. These observations, along with literature data, indicated the importance of vibrational correction. Indeed, the inclusion of perturbative vibrational correction (revPBE0/def2-TZVPP) reduces relative errors of the DLPNO-CCSD calculation to 3-8%, and the correlation of the calculated and the experimental $^{14}N$ $a_{iso}$ (Fig. 4, red) readily becomes almost linear. The remaining errors of 0.3-1.3G (MAD = 0.8 G) originate from several small contributions. First, DFT calculation probably underestimates vibrational correction (see Auer et al. [67]). On the other hand, the inclusion of only the harmonic contribution probably leads to the overestimation of vibrational correction, especially in the *3-imidazoline-3-oxide-oxyl* series. Secondly, deviation of DLPNO-CCSD results from canonical CCSD results [5] and the lack of triples correction [16] further draw calculated values away from the experiment. Finally, error from incompletion of the basis set and approximate way of the solvent's inclusion in the calculation may also contribute to deviation from the experiment. Some of these errors are covered in the papers by Barone et al. [16, 69–71]. The divergence between DLPNO-CCSD calculation and experimental spin-dipole contribution to hyperfine coupling tensor ($A^{dd}_z$), which is already relatively small (MAD = 0.5 G), further benefits from the inclusion of the vibrational correction (MAD = 0.3 G). In general DLPNO-CCSD method with the perturbative harmonic vibrational correction ($a_{iso}$ MAD = 0.8 G, $A^{dd}_z$ MAD = 0.3 G) outperforms most DFT methods (vide infra) and should be preferred even in routine usage.

**Table 1** $^{14}N$ isotropic hyperfine coupling constants of nitroxide radicals VI- LXXVIII ($a_{iso}$) and the diagonal element of spin-dipole contribution to hyperfine coupling tensor ($A^{dd}_z$) calculated using the DLPNO-CCSD method and respective absolute errors (AE) compared with the experiment. The vibrational correction ($\Delta a_{iso}^{vib}$ and $\Delta A^{dd}_{z}{}^{vib}$) is estimated at revPBE0/def2-TZVPP level

| Radical | $\Delta a_{iso}^{vib}$ (0 K/140K) | $a_{iso}$ DLPNO-CCSD | $a_{iso}$ DLPNO-CCSD corrected | $a_{iso}$ exp* | $AE_{iso}$ *uncorrected /corrected* | $\Delta A^{dd}{}_z^{vib}$ (0 K/140K) | $A^{dd}{}_z$ DLPNO-CCSD | $A^{dd}{}_z$ DLPNO-CCSD corrected | $A^{dd}{}_z$ Exp | $AE_{dd}$ *uncorrected /corrected* |
|---|---|---|---|---|---|---|---|---|---|---|
| *Piperidine series* | | | | | | | | | | |
| VI | 0.3/0.4 | 14.6 | 14.9 | 15.7 | 1.2/0.8 | -0.1/-0.1 | 18.0 | 17.9 | 18.3 | 0.2/0.4 |
| VII | 0.3/0.3 | 14.6 | 14.9 | 15.8 | 1.3/1.0 | -0.2/-0.2 | 18.5 | 18.3 | 18.4 | 0.1/0.1 |
| VIII | 0.4/0.5 | 14.4 | 14.9 | 16.1 | 1.7/1.3 | -0.1/-0.1 | 18.3 | 18.2 | 18.7 | 0.4/0.5 |
| X | 0.3/0.3 | 14.5 | 14.9 | 15.9 | 1.4/1.0 | -0.2/-0.2 | 18.3 | 18.2 | 18.1 | 0.2/0.1 |
| XIII | 0.3/0.3 | 14.5 | 14.8 | 15.8 | 1.4/1.0 | -0.2/-0.2 | 18.4 | 18.2 | 18.5 | 0.1/0.3 |
| XV | 0.3/0.3 | 14.3 | 14.6 | 15.8 | 1.5/1.2 | -0.2/-0.2 | 18.5 | 18.3 | 17.7 | 0.8/0.6 |
| XIX | 0.3/0.3 | 14.3 | 14.6 | 15.5 | 1.2/0.9 | -0.1/-0.2 | 18.0 | 17.9 | 17.9 | 0.1/0.0 |
| XX | 0.3/0.3 | 14.4 | 14.7 | 15.7 | 1.3/1.0 | -0.1/-0.2 | 18.0 | 17.8 | 18.1 | 0.1/0.3 |
| *Pyrroline series* | | | | | | | | | | |
| XXXVII | 1.3/1.6 | 12.0 | 13.6 | 14.7 | 2.8/1.1 | -0.4/-0.4 | 19.7 | 19.3 | 19.3 | 0.4/0.0 |
| *Imidazoline series* | | | | | | | | | | |
| XLIV | 1.4/1.9 | 11.5 | 13.4 | 14.0 | 2.5/0.6 | -0.4/-0.5 | 19.3 | 18.8 | 18.4 | 1.0/0.5 |
| *3-imidazoline-3-oxide-oxyl series* | | | | | | | | | | |
| LII | 2.3/2.9 | 11.0 | 13.9 | 14.1 | 3.2/0.3 | -0.6/-0.7 | 19.2 | 18.4 | 18.1 | 1.1/0.4 |
| LIII | 1.1/1.6 | 11.5 | 13.1 | 13.9 | 2.4/0.8 | -0.3/-0.4 | 19.1 | 18.7 | 18.6 | 0.5/0.1 |
| LIX | 1.9/2.5 | 11.0 | 13.5 | 14.0 | 3.0/0.5 | -0.5/-0.6 | 19.2 | 18.5 | 18.2 | 0.9/0.3 |
| LX | 1.9/2.5 | 11.0 | 13.4 | 14.0 | 3.0/0.5 | -0.5/-0.6 | 19.2 | 18.6 | 18.3 | 0.8/0.2 |
| LXI | 1.9/2.5 | 11.0 | 13.4 | 14.0 | 3.0/0.5 | -0.5/-0.6 | 19.0 | 18.4 | 18.2 | 0.8/0.2 |
| LXII | 0.8/1.1 | 12.2 | 13.2 | 14.1 | 1.9/0.8 | -0.2/-0.3 | 18.7 | 18.4 | 18.0 | 0.7/0.4 |
| *Pyrrolidine series* | | | | | | | | | | |
| LXVII | 0.9/1.4 | 12.1 | 13.5 | 14.0 | 1.9/0.5 | -0.3/-0.4 | 19.5 | 19.1 | 19.0 | 0.5/0.1 |
| LXVIII | 1.1/1.6 | 11.5 | 13.1 | 14.0 | 2.5/0.9 | -0.3/-0.4 | 19.3 | 18.9 | 19.3 | 0.0/0.4 |
| *Imidazolidine series* | | | | | | | | | | |
| LXX | 0.5/0.6 | 13.4 | 14.0 | 15.1 | 1.6/1.1 | -0.2/-0.2 | 18.6 | 18.5 | 18.1 | 0.5/0.3 |
| LXXI | 0.5/0.6 | 13.5 | 14.0 | 14.7 | 1.2/0.7 | -0.2/-0.2 | 18.4 | 18.2 | 18.1 | 0.4/0.2 |
| LXXII | 0.5/0.5 | 13.8 | 14.3 | 15.5 | 1.8/1.2 | -0.2/-0.2 | 18.4 | 18.2 | 18.1 | 0.3/0.1 |
| LXXIV | 0.4/0.5 | 14.2 | 14.7 | 15.5 | 1.3/0.8 | -0.2/-0.2 | 18.3 | 18.1 | 17.4 | 0.9/0.7 |
| LXXVIII | 0.8/0.9 | 12.5 | 13.4 | 13.9 | 1.4/0.5 | -0.2/-0.3 | 19.1 | 18.8 | 18.7 | 0.4/0.1 |

* values calculated as an average of the diagonal elements ($A_n$) of the hyperfine coupling tensors

### 3.2 DFT calculation

Our previous paper mentioned a slightly controversial trend: description of $^{14}N$ isotropic HFC in nitroxide radicals by DFT functionals generally follows pattern noted by Medvedev et al. [2]. In contrast, the description of the dipole-dipole contribution to $^{14}N$ HFC is

strongly inconsistent with that pattern.

Whenever calculated vibrationally corrected $^{14}N$ $a_{iso}$ are compared with experimental values or calculated with DLPNO-CCSD values, the best agreement with the reference is brought by hybrid mGGA functionals (TPSS0, M06, M06-2X) and the double hybrid GGA functional B2PLYP. Next come hybrid GGA functionals (PBE0, B97, and B98). On the other hand, the worst performance is delivered by GGA functionals (PBE, BP86, e.t.c). Here one should note several interesting things. The M06 functional, which performed best without vibrational correction, still yields calculated $a_{iso}$ values in good agreement with the experiment (MAD = 0.7 G). However, agreement with the DLPNO-CCSD reference values is significantly worse (MAD = 1.4 G) than with the experimental reference. In contrast with the correlation of DLPNO-CCSD calculated values and experimental values, which becomes more linear after applying the vibrational correction, corrected M06 results behave opposite (Fig. 4) and deviate significantly from any linear trend. It worth noting that in contrast to the M06 functional results, values calculated using the TPSS0 functional strongly benefit from the inclusion of the vibrational correction with both decreased MAD and the calculated v. experimental correlation became closer to a linear trend (Fig. 4). The TPSS0 and B2PLYP functionals also deliver results in the closest agreement with the DLPNO-CCSD method.

One of the most notorious disagreements with Medvedev et al. [2] results is the results delivered by SCAN and hybrid SCAN0 functionals, well performed in electron density. Along with MN15 functional, they bring $^{14}N$ $a_{iso}$ values, which are sometimes more than 100% off from experimental values. It is not the first observation of the SCAN-family functionals' poor performance in HFC calculation. For example, Witwicki et al. [5] found that calculation of $^{1}H$ $a^{iso}$ in o-semiquinonato $Mg^{2+}$ complex using SCAN functional might predict the wrong sign of the coupling constant. Earlier Pantazis [15] noted that sometimes the SCAN-family functionals yield erroneous results in transition metals coordination compounds HFCC calculation. It was explained by the calculation converging to a wrong state. In the present calculation, both general spin density distribution and $A^{dd}_{z}$ calculated by the SCAN-family functionals and the MN15 functional do not deviate significantly from those calculated using any other functional (Fig. 5). Finally, it is interesting to note that the B3LYP/N07D functional/basis combination, which is frequently used for routine EPR calculations due to its low computational cost and accuracy, strongly suffers from the inclusion of the vibrational correction as its $a_{iso}$ mean absolute deviation from the experiment doubles (1.0 G without correction and 2.0 G with correction). Simultaneously, the mean absolute deviation from the DLPNO-CCSD reference is as big as 2.9 G. In general, most DFT functionals used here underestimate Fermi contact contribution to $^{14}N$ $a_{iso}$ and thus benefit from the inclusion of the vibrational correction, which is positive for the radicals used here. Therefore, mean deviations from the experiment are almost uniformly decreased by 1.1 G, and the DFT functionals ranking by their accuracy in $^{14}N$ $a_{iso}$ prediction are practically not affected by the inclusion of the vibrational correction, except for the M06-family functionals, which slightly underestimated $^{14}N$ $a_{iso}$ before correction and slightly overestimated it after correction. The BHandHLYP and M06L functionals, the B3LYP/N07D and PBE0/N07D functional/basis set combinations are the only methods to increase their deviation from the experiment after inclusion of the correction.

On the other hand, the performance of DFT methods in the spin dipole contribution to 14N HFCC calculation (here $A^{dd}_{z}$ component is used) contradicts the trends in electron density and Fermi contact contribution to HFCC. The best performers are the GGA and mGGA functionals (OLYP, PBE, PBEpow, PBEGXPBE, TPSS) and the M06-family functionals. The mainstream hybrid GGA and mGGA functionals (PBE0, B97, TPSS0) perform slightly worse. In general, we should note that the major part of the DFT functionals used here deal with the spin dipole contribution better than with Fermi contact contribution to $^{14}N$ HFCC, which is also known from the literature [5, 72]. Though this is not necessarily always so, see, for example, Kossmann et al. [7].

**Table 2** Mean absolute deviations (in G) for calculated $^{14}N$ $a_{iso}$ and $A^{dd}_{z}$ versus the experimental values and versus the values, calculated with the DLPNO-CCSD method. ,

| Method | $a_{iso}$ | $a_{iso}$ v. DLPNO-CCSD | $a_{iso}$ corrected | $A^{dd}_z$ | $A^{dd}_z$ v. DLPNO-CCSD | $A^{dd}_z$ corrected | Method class Method Year |
|---|---|---|---|---|---|---|---|
| M062X | 0.6 | 1.3 | 0.5 | 0.4 | 0.2 | 0.2 | hmGGA, 2008 |
| M06 | 0.6 | 1.4 | 0.7 | 0.4 | 0.1 | 0.2 | hmGGA, 2008 |
| **DLPNO-CCSD** | 1.9 | 0.0 | 0.8 | 0.5 | 0.0 | 0.3 | WFT, 2018 |
| B2PLYP | 2.1 | 0.3 | 1.0 | 1.5 | 1.1 | 1.2 | dhGGA, 2006 |
| TPSS0 | 2.3 | 0.4 | 1.2 | 1.2 | 0.7 | 0.8 | hmGGA, 2003 |
| B97 | 2.9 | 1.0 | 1.9 | 0.9 | 0.4 | 0.5 | hGGA, 1997 |
| B98 | 3.0 | 1.1 | 1.9 | 1.0 | 0.6 | 0.7 | hmGGA, 1998 |
| BHandHLYP | 0.9 | 2.8 | 2.0 | 1.7 | 1.3 | 1.4 | hGGA, 1993 |
| PBE0 | 3.1 | 1.2 | 2.0 | 1.1 | 0.7 | 0.8 | hGGA, 1999 |
| *B3LYP/N07D* | 1.0 | 2.9 | 2.0 | 1.1 | 1.5 | 1.4 | hGGA, 2008 |
| MN15L | 3.5 | 1.6 | 2.4 | 1.0 | 1.4 | 1.3 | mGGA, 2016 |
| B3LYP | 3.6 | 1.6 | 2.5 | 1.4 | 1.0 | 1.1 | hGGA, 1994 |
| mPW1PW | 3.7 | 1.7 | 2.6 | 1.2 | 0.8 | 0.9 | hGGA, 1998 |
| CAM-B3LYP | 3.7 | 1.8 | 2.6 | 1.6 | 1.2 | 1.3 | RS-hGGA, 2004 |
| *PBE0/N07D* | 1.8 | 3.7 | 2.9 | 1.3 | 1.7 | 1.6 | hGGA, 2008 |
| wB97x | 4.0 | 2.1 | 2.9 | 0.9 | 0.5 | 0.6 | RS-hGGA, 2008 |
| PBEGXPBE | 4.1 | 2.1 | 3.0 | 0.4 | 0.1 | 0.2 | mGGA, 2017 |
| PBE1KCIS | 5.0 | 3.1 | 3.9 | 0.9 | 0.5 | 0.6 | hmGGA, 2005 |
| TPSS | 5.2 | 3.3 | 4.1 | 0.8 | 0.4 | 0.5 | mGGA, 2003 |
| M06L | 3.2 | 5.2 | 4.3 | 0.4 | 0.1 | 0.2 | mGGA, 2006 |
| OLYP | 5.7 | 3.7 | 4.6 | 0.3 | 0.3 | 0.3 | GGA, 2001 |
| PBEPOW | 5.9 | 3.9 | 4.8 | 0.4 | 0.1 | 0.2 | GGA, 2016 |
| PBE | 6.2 | 4.2 | 5.1 | 0.7 | 0.2 | 0.4 | GGA, 1996 |
| BP86 | 6.9 | 5.0 | 5.8 | 0.8 | 0.4 | 0.5 | GGA, 1988 |
| BEEF | 8.6 | 6.7 | 7.5 | 0.9 | 0.5 | 0.6 | GGA, 2012 |
| HSE06 | 11.1 | 9.2 | 10.0 | 2.0 | 2.4 | 2.3 | hGGA, 2006 |
| SCAN0 | 12.6 | 10.7 | 11.5 | 1.7 | 1.3 | 1.4 | hmGGA, 2016 |
| SCAN | 17.9 | 16.0 | 16.8 | 1.6 | 1.2 | 1.3 | mGGA, 2015 |
| MN15 | 19.2 | 17.2 | 18.1 | 0.6 | 1.0 | 0.9 | hmGGA, 2016 |

In the previous paper [6], we have already discussed that M06-family functionals, while outperforming other DFT methods in calculating the $^{14}N$ HFC of the present radicals set, may in many cases fail to compete with other common functionals like TPSS0 or B2PLYP [5, 14]. In a broader perspective, TPSS0 and B2PLYP functionals remain the most reliable choice for an HFC calculation in the DFT framework. For example, when the DLPNO-CCSD method's routine use in a preliminary experimental data interpretation by a brute force search of a suitable radical or calculation of large radicals' vibrational corrections and in other applications is too demanding.

# Conclusions

In the present study, we have evaluated the performance of 26 different DFT functionals in conjunction with the harmonic contribution to the perturbative vibrational correction in the spin density calculating of a set of 23 nitroxide radicals and compared their results against the experiment and the results DLPNO-CCSD calculation. $^{14}$N hyperfine coupling was used as a natural descriptor of the spin density.

The DLPNO-CCSD method outperformed most DFT methods with a mean absolute deviation from the experiment of 0.8 G in $a_{iso}$ (i.e., Fermi contact coupling contribution) and 0.3 G in $A^{dd}_z$ (i.e., spin dipole contribution) after vibrational correction. The use of vibrational correction also significantly linearized the correlation of the experimental and calculated values. The best results in DFT functionals are obtained using the M06-2X/COSMO and M06/COSMO methods with MAD of 0.5 G and 0.7 G respectively in $a_{iso}$ and MAD = 0.2 G and 0.2 G in $A^{dd}_z$. The SCAN, SCAN0, and MN15 functionals were found to be the worst performers with relative errors in $a_{iso}$ up to 100% or even more. Otherwise, the trends in the spin density description by DFT methods follow tendencies observed earlier in the electron density description.

We have found that the calculation of $^{14}$N HFC in most DFT functionals significantly benefit from vibrational correction. MAD in $a_{iso}$ is reduced thus by 1.1 G, corresponding to a relative error reduction of about 7.4 %. The only exceptions among functionals used are the M06-family functionals and the BHandHLYP. The well-known N07D scheme also, while being quite successful without the vibrational correction (MAD($A^{dd}_z$) = 0.5 G and MAD($a_{iso}$) = 1.0 G for the B3LYP/N07D/COSMO method), yields results stronger deviating from experiment upon application of the correction (MAD($A^{dd}_z$) = 1.4 G and MAD($a_{iso}$) = 2.0 G for the B3LYP/N07D/COSMO method).

# Declarations

Supporting Information: A table containing calculated HFC tensor components in CSV format.

**Acknowledgments** The research is supported by Russian Foundation for Basic Research (Grant 18-33-00866 mol_a); calculations were performed using resources of the Supercomputing Center of the Lomonosov Moscow State University [73]

### Conflict of interest

The author declares no competing interests.

### Availability of data and material

All data generated or analysed during this study are included in this published article (and its supplementary information files).

### Code availability

The code used in the study is mentioned in this article and can be obtained from its official website

### Authors' contributions

N/A

# References

1. Mardirossian N, Head-Gordon M (2017) Thirty years of density functional theory in computational chemistry: an overview and extensive assessment of 200 density functionals. Mol Phys 115:2315–2372. https://doi.org/10.1080/00268976.2017.1333644
2. Medvedev MG, Bushmarinov IS, Sun J, et al (2017) Density functional theory is straying from the path toward the exact functional. Science (80- ) 355:49–52. https://doi.org/10.1126/science.aah5975
3. Marjewski AA, Medvedev MG, Gerasimov IS, et al (2018) Interplay between test sets and statistical procedures in ranking DFT methods: The case of electron density studies. Mendeleev Commun 28:225–235. https://doi.org/10.1016/j.mencom.2018.05.001
4. Hait D, Head-Gordon M (2018) How Accurate Is Density Functional Theory at Predicting Dipole Moments? An Assessment Using a New Database of 200 Benchmark Values. J Chem Theory Comput 14:1969–1981. https://doi.org/10.1021/acs.jctc.7b01252
5. Witwicki M, Walencik PK, Jezierska J (2020) How accurate is density functional theory in predicting spin density? An insight from the prediction of hyperfine coupling constants. J Mol Model 26:10. https://doi.org/10.1007/s00894-019-4268-0
6. Gromov OI, Kuzin S V., Golubeva EN (2019) Performance of DFT methods in the calculation of isotropic and dipolar contributions to 14N hyperfine coupling constants of nitroxide radicals. J Mol Model 25:93. https://doi.org/10.1007/s00894-019-3966-y
7. Kossmann S, Kirchner B, Neese F (2007) Performance of modern density functional theory for the prediction of hyperfine structure: meta-GGA and double hybrid functionals. Mol Phys 105:2049–2071. https://doi.org/10.1080/00268970701604655
8. Weil JA, Bolton JR (2006) Electron Paramagnetic Resonance. John Wiley & Sons, Inc., Hoboken, NJ, USA
9. Hermosilla L, Calle P, García de la Vega JM, Sieiro C (2005) Theoretical Isotropic Hyperfine Coupling Constants of Third-Row Nuclei ( 29 Si, 31 P, and 33 S). J Phys Chem A 109:7626–7635. https://doi.org/10.1021/jp0522361
10. Hermosilla L, Calle P, García de la Vega JM, Sieiro C (2005) Density Functional Theory Predictions of Isotropic Hyperfine Coupling Constants. J Phys Chem A 109:1114–1124. https://doi.org/10.1021/jp0466901
11. Hermosilla L, Calle P, García de la Vega JM, Sieiro C (2006) Density Functional Theory Study of 14 N Isotropic Hyperfine Coupling Constants of Organic Radicals. J Phys Chem A 110:13600–13608. https://doi.org/10.1021/jp064900z
12. Hermosilla L, Vega JMG de la, Sieiro C, Calle P (2011) DFT Calculations of Isotropic Hyperfine Coupling Constants of Nitrogen Aromatic Radicals: The Challenge of Nitroxide Radicals. J Chem Theory Comput 7:169–179. https://doi.org/10.1021/ct1006136
13. Hermosilla L, Calle P, García de la Vega JM (2015) Modeling EPR parameters of nitrogen containing conjugated radical cations. RSC Adv 5:62551–62562. https://doi.org/10.1039/C5RA08758A
14. Witwicki M (2018) Density functional theory and ab initio studies on hyperfine coupling constants of phosphinyl radicals. Int J Quantum Chem 118:e25779. https://doi.org/10.1002/qua.25779
15. Pantazis DA (2019) First-Principles Calculation of Transition Metal Hyperfine Coupling Constants with the Strongly Constrained and Appropriately Normed (SCAN) Density Functional and its Hybrid Variants. Magnetochemistry 5:69. https://doi.org/10.3390/magnetochemistry5040069
16. Puzzarini C, Barone V (2009) Theoretical Study of the $X_2$ NO Systems (X = F, Cl, Br, I): Effects of Halogen Substitution on Structural and Spectroscopic Properties. J Chem Theory Comput 5:2378–2387. https://doi.org/10.1021/ct9001762
17. Saitow M, Neese F (2018) Accurate spin-densities based on the domain-based local pair-natural orbital coupled-cluster theory. J Chem Phys 149:034104. https://doi.org/10.1063/1.5027114
18. Neese F (2018) Software update: the ORCA program system, version 4.0. Wiley Interdiscip Rev Comput Mol Sci 8:e1327. https://doi.org/10.1002/wcms.1327
19. Karton A, Tarnopolsky A, Lamère J-F, et al (2008) Highly Accurate First-Principles Benchmark Data Sets for the Parametrization and Validation of Density Functional and Other Approximate Methods. Derivation of a Robust, Generally Applicable, Double-Hybrid Functional for Thermochemistry and Thermochemical Kinetics †. J Phys Chem A 112:12868–12886. https://doi.org/10.1021/jp801805p
20. Weigend F, Ahlrichs R (2005) Balanced basis sets of split valence, triple zeta valence and quadruple zeta valence quality for H to Rn: Design and assessment of accuracy. Phys Chem Chem Phys 7:3297. https://doi.org/10.1039/b508541a
21. Sinnecker S, Rajendran A, Klamt A, et al (2006) Calculation of Solvent Shifts on Electronic g -Tensors with the Conductor-Like Screening Model (COSMO) and Its Self-Consistent Generalization to Real Solvents (Direct COSMO-RS). J Phys Chem A 110:2235–2245. https://doi.org/10.1021/jp056016z
22. Brémond É, Savarese M, Su NQ, et al (2016) Benchmarking Density Functionals on Structural Parameters of Small-/Medium-Sized Organic Molecules. J Chem Theory Comput 12:459–465. https://doi.org/10.1021/acs.jctc.5b01144

23. Lehtola S, Steigemann C, Oliveira MJT, Marques MAL (2018) Recent developments in LIBXC — A comprehensive library of functionals for density functional theory. SoftwareX 7:1–5. https://doi.org/10.1016/j.softx.2017.11.002
24. Sun J, Ruzsinszky A, Perdew J (2015) Strongly Constrained and Appropriately Normed Semilocal Density Functional. Phys Rev Lett 115:036402. https://doi.org/10.1103/PhysRevLett.115.036402
25. Mezei PD, Csonka GI, Kállay M (2018) Simple Modifications of the SCAN Meta-Generalized Gradient Approximation Functional. J Chem Theory Comput 14:2469–2479. https://doi.org/10.1021/acs.jctc.8b00072
26. Hui K, Chai J-D (2016) SCAN-based hybrid and double-hybrid density functionals from models without fitted parameters. J Chem Phys 144:044114. https://doi.org/10.1063/1.4940734
27. Wellendorff J, Lundgaard KT, Møgelhøj A, et al (2012) Density functionals for surface science: Exchange-correlation model development with Bayesian error estimation. Phys Rev B - Condens Matter Mater Phys 85:. https://doi.org/10.1103/PhysRevB.85.235149
28. Brémond É (2016) A power series revisit of the PBE exchange density-functional approximation: The PBEpow model. J Chem Phys 145:. https://doi.org/10.1063/1.4972815
29. Perdew JP, Burke K, Ernzerhof M (1996) Generalized Gradient Approximation Made Simple. Phys Rev Lett 77:3865–3868. https://doi.org/10.1103/PhysRevLett.77.3865
30. Loos PF (2017) Exchange functionals based on finite uniform electron gases. J Chem Phys 146:. https://doi.org/10.1063/1.4978409
31. Yu HS, He X, Li SL, Truhlar DG (2016) MN15: A Kohn-Sham global-hybrid exchange-correlation density functional with broad accuracy for multi-reference and single-reference systems and noncovalent interactions. Chem Sci 7:5032–5051. https://doi.org/10.1039/c6sc00705h
32. Yu HS, He X, Truhlar DG (2016) MN15-L: A New Local Exchange-Correlation Functional for Kohn–Sham Density Functional Theory with Broad Accuracy for Atoms, Molecules, and Solids. J Chem Theory Comput 12:1280–1293. https://doi.org/10.1021/acs.jctc.5b01082
33. Zhao Y, Truhlar DG (2005) Benchmark Databases for Nonbonded Interactions and Their Use To Test Density Functional Theory. J Chem Theory Comput 1:415–432. https://doi.org/10.1021/ct049851d
34. Krieger JB, Chen J, Iafrate GJ, Savin A (1999) Construction of An Accurate Self-interaction-corrected Correlation Energy Functional Based on An Electron Gas with A Gap. In: Electron Correlations and Materials Properties. Springer US, Boston, MA, pp 463–477
35. Heyd J, Scuseria GE, Ernzerhof M (2003) Hybrid functionals based on a screened Coulomb potential. J Chem Phys 118:8207–8215. https://doi.org/10.1063/1.1564060
36. Schmider HL, Becke AD (1998) Optimized density functionals from the extended G2 test set. J Chem Phys 108:9624–9631. https://doi.org/10.1063/1.476438
37. Perdew JP (1986) Density-functional approximation for the correlation energy of the inhomogeneous electron gas. Phys Rev B 33:8822–8824. https://doi.org/10.1103/PhysRevB.33.8822
38. Becke AD (1988) Density-functional exchange-energy approximation with correct asymptotic behavior. Phys Rev A 38:3098–3100. https://doi.org/10.1103/PhysRevA.38.3098
39. Hoe W-M, Cohen AJ, Handy NC (2001) Assessment of a new local exchange functional OPTX. Chem Phys Lett 341:319–328. https://doi.org/10.1016/S0009-2614(01)00581-4
40. Staroverov VN, Scuseria GE, Tao J, Perdew JP (2003) Comparative assessment of a new nonempirical density functional: Molecules and hydrogen-bonded complexes. J Chem Phys 119:12129–12137. https://doi.org/10.1063/1.1626543
41. Zhao Y, Truhlar DG (2006) A new local density functional for main-group thermochemistry, transition metal bonding, thermochemical kinetics, and noncovalent interactions. J Chem Phys 125:194101. https://doi.org/10.1063/1.2370993
42. Stephens PJ, Devlin FJ, Chabalowski CF, Frisch MJ (1994) Ab Initio Calculation of Vibrational Absorption and Circular Dichroism Spectra Using Density Functional Force Fields. J Phys Chem 98:11623–11627. https://doi.org/10.1021/j100096a001
43. Adamo C, Barone V (1999) Toward reliable density functional methods without adjustable parameters: The PBE0 model. J Chem Phys 110:6158–6170. https://doi.org/10.1063/1.478522
44. Adamo C, Barone V (1998) Exchange functionals with improved long-range behavior and adiabatic connection methods without adjustable parameters: The mPW and mPW1PW models. J Chem Phys 108:664–675. https://doi.org/10.1063/1.475428

45. Becke AD (1997) Density-functional thermochemistry. V. Systematic optimization of exchange-correlation functionals. J Chem Phys 107:8554–8560. https://doi.org/10.1063/1.475007
46. Becke AD (1993) A new mixing of Hartree–Fock and local density-functional theories. J Chem Phys 98:1372–1377. https://doi.org/10.1063/1.464304
47. Zhao Y, Truhlar DG (2008) The M06 suite of density functionals for main group thermochemistry, thermochemical kinetics, noncovalent interactions, excited states, and transition elements: two new functionals and systematic testing of four M06-class functionals and 12 other function. Theor Chem Acc 120:215–241. https://doi.org/10.1007/s00214-007-0310-x
48. Tawada Y, Tsuneda T, Yanagisawa S, et al (2004) A long-range-corrected time-dependent density functional theory. J Chem Phys 120:8425–8433. https://doi.org/10.1063/1.1688752
49. Chai J-D, Head-Gordon M (2008) Systematic optimization of long-range corrected hybrid density functionals. J Chem Phys 128:084106. https://doi.org/10.1063/1.2834918
50. Grimme S (2006) Semiempirical hybrid density functional with perturbative second-order correlation. J Chem Phys 124:034108. https://doi.org/10.1063/1.2148954
51. Barone V, Cimino P (2008) Accurate and feasible computations of structural and magnetic properties of large free radicals: The PBE0/N07D model. Chem Phys Lett 454:139–143. https://doi.org/10.1016/j.cplett.2008.01.080
52. Barone V, Cimino P, Stendardo E (2008) Development and Validation of the B3LYP/N07D Computational Model for Structural Parameter and Magnetic Tensors of Large Free Radicals. J Chem Theory Comput 4:751–764. https://doi.org/10.1021/ct800034c
53. Datta D, Gauss J (2019) Accurate Prediction of Hyperfine Coupling Tensors for Main Group Elements Using a Unitary Group Based Rigorously Spin-Adapted Coupled-Cluster Theory. J Chem Theory Comput 15:1572–1592. https://doi.org/10.1021/acs.jctc.8b01048
54. Peterson KA, Dunning TH (2002) Accurate correlation consistent basis sets for molecular core-valence correlation effects: The second row atoms Al-Ar, and the first row atoms B-Ne revisited. J Chem Phys 117:10548–10560. https://doi.org/10.1063/1.1520138
55. Provasi PF, Aucar GA, Sauer SPA (2001) The effect of lone pairs and electronegativity on the indirect nuclear spin–spin coupling constants in CH2X (X=CH2, NH, O, S): Ab initio calculations using optimized contracted basis sets. J Chem Phys 115:1324–1334. https://doi.org/10.1063/1.1379331
56. Jakobsen P, Jensen F (2019) Probing basis set requirements for calculating hyperfine coupling constants. J Chem Phys 151:174107. https://doi.org/10.1063/1.5128286
57. Neese F, Wennmohs F, Hansen A, Becker U (2009) Efficient, approximate and parallel Hartree–Fock and hybrid DFT calculations. A 'chain-of-spheres' algorithm for the Hartree–Fock exchange. Chem Phys 356:98–109. https://doi.org/10.1016/j.chemphys.2008.10.036
58. Stoychev GL, Auer AA, Neese F (2017) Automatic Generation of Auxiliary Basis Sets. J Chem Theory Comput 13:554–562. https://doi.org/10.1021/acs.jctc.6b01041
59. Barone V, Cimino P, Pedone A (2010) An integrated computational protocol for the accurate prediction of EPR and PNMR parameters of aminoxyl radicals in solution. Magn Reson Chem 48:S11–S22. https://doi.org/10.1002/mrc.2640
60. Datta D, Kossmann S, Neese F (2016) Analytic energy derivatives for the calculation of the first-order molecular properties using the domain-based local pair-natural orbital coupled-cluster theory. J Chem Phys 145:114101. https://doi.org/10.1063/1.4962369
61. Saitow M, Becker U, Riplinger C, et al (2017) A new near-linear scaling, efficient and accurate, open-shell domain-based local pair natural orbital coupled cluster singles and doubles theory. J Chem Phys 146:164105. https://doi.org/10.1063/1.4981521
62. Åstrand P-O, Ruud K, Taylor PR (2000) Calculation of the vibrational wave function of polyatomic molecules. J Chem Phys 112:2655–2667. https://doi.org/10.1063/1.480840
63. Chen X, Rinkevicius Z, Cao Z, et al (2011) Zero-point vibrational corrections to isotropic hyperfine coupling constants in polyatomic molecules. Phys Chem Chem Phys 13:696–707. https://doi.org/10.1039/C0CP01443E
64. Mort BC, Autschbach J (2005) Magnitude of Zero-Point Vibrational Corrections to Optical Rotation in Rigid Organic Molecules: A Time-Dependent Density Functional Study. J Phys Chem A 109:8617–8623. https://doi.org/10.1021/jp051685y
65. Egidi F, Bloino J, Cappelli C, et al (2013) Tuning of NMR and EPR parameters by vibrational averaging and environmental effects: an integrated computational approach. Mol Phys 111:1345–1354. https://doi.org/10.1080/00268976.2013.796413

66. Bloino J, Barone V (2012) A second-order perturbation theory route to vibrational averages and transition properties of molecules: General formulation and application to infrared and vibrational circular dichroism spectroscopies. J Chem Phys 136:124108. https://doi.org/10.1063/1.3695210
67. Auer AA, Tran VA, Sharma B, et al (2020) A case study of density functional theory and domain-based local pair natural orbital coupled cluster for vibrational effects on EPR hyperfine coupling constants: vibrational perturbation theory versus ab initio molecular dynamics. Mol Phys e1797916. https://doi.org/10.1080/00268976.2020.1797916
68. Lebedev YS, Grinberg OY, Dubinsky AA, Poluektov OG (1992) Investigation of Spin Labels and Probes by Millimeter Band EPR. In: Bioactive Spin Labels. Springer Berlin Heidelberg, Berlin, Heidelberg, pp 227–278
69. Puzzarini C, Barone V (2008) Toward spectroscopic accuracy for organic free radicals: Molecular structure, vibrational spectrum, and magnetic properties of F2NO. J Chem Phys 129:084306. https://doi.org/10.1063/1.2969820
70. Barone V, Biczysko M, Bloino J, et al (2013) Accurate structure, thermodynamics, and spectroscopy of medium-sized radicals by hybrid coupled cluster/density functional theory approaches: The case of phenyl radical. J Chem Phys 138:234303. https://doi.org/10.1063/1.4810863
71. Puzzarini C, Barone V (2010) Toward spectroscopic accuracy for open-shell systems: Molecular structure and hyperfine coupling constants of H2CN, H2CP, NH2, and PH2 as test cases. J Chem Phys 133:184301. https://doi.org/10.1063/1.3503763
72. Hedegård ED, Kongsted J, Sauer SPA (2012) Improving the calculation of electron paramagnetic resonance hyperfine coupling tensors for d-block metals. Phys Chem Chem Phys 14:10669. https://doi.org/10.1039/c2cp40969k
73. Sadovnichy V, Tikhonravov A, Voevodin V, Opanasenko V (2013) “Lomonosov”: Supercomputing at Moscow State University. In: Vetter JS (ed) Contemporary High Performance Computing: From Petascale toward Exascale. CRC Press, Boca Raton, pp 283–307

## Figures

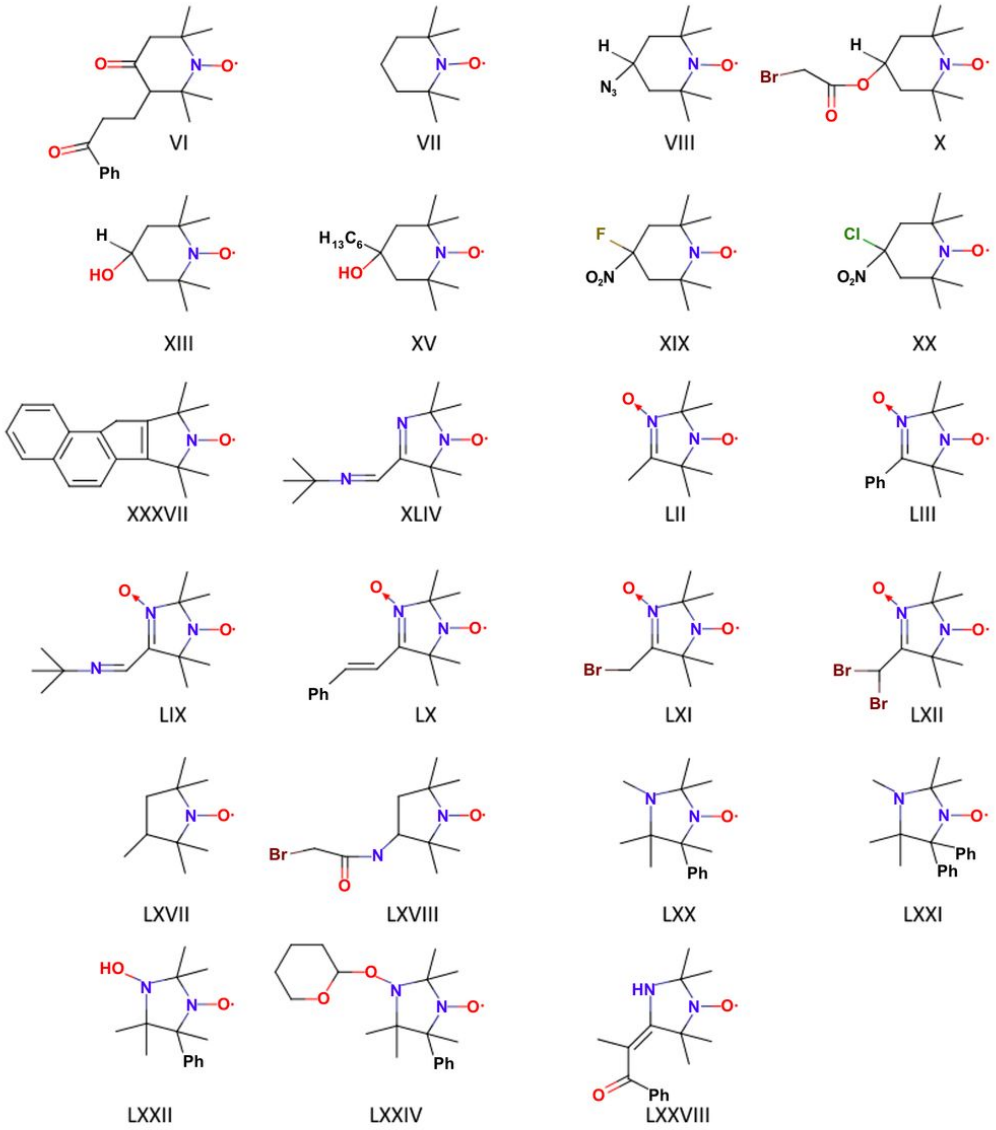


## Figure 1

Nitroxide radicals used in the present study [68]

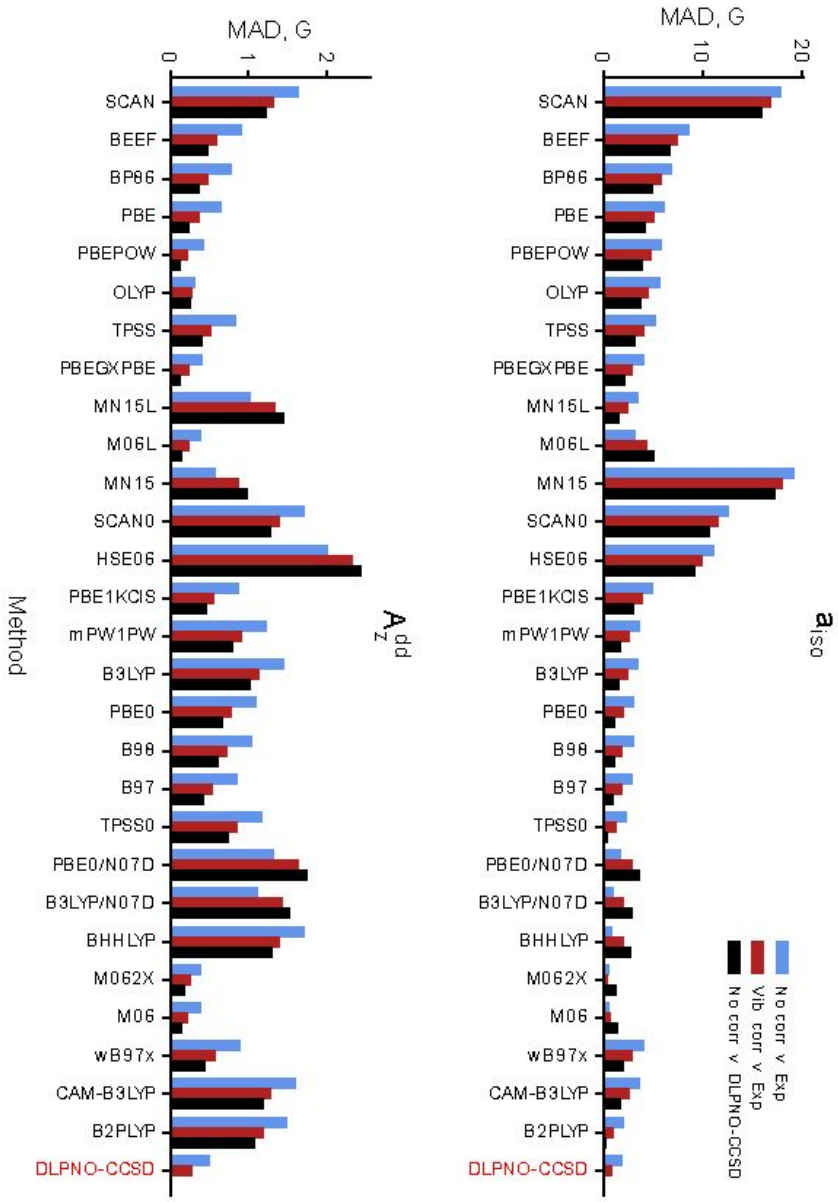


## Figure 2

Due to technical limitations, the caption for Figure 2 is only available in the manuscript.

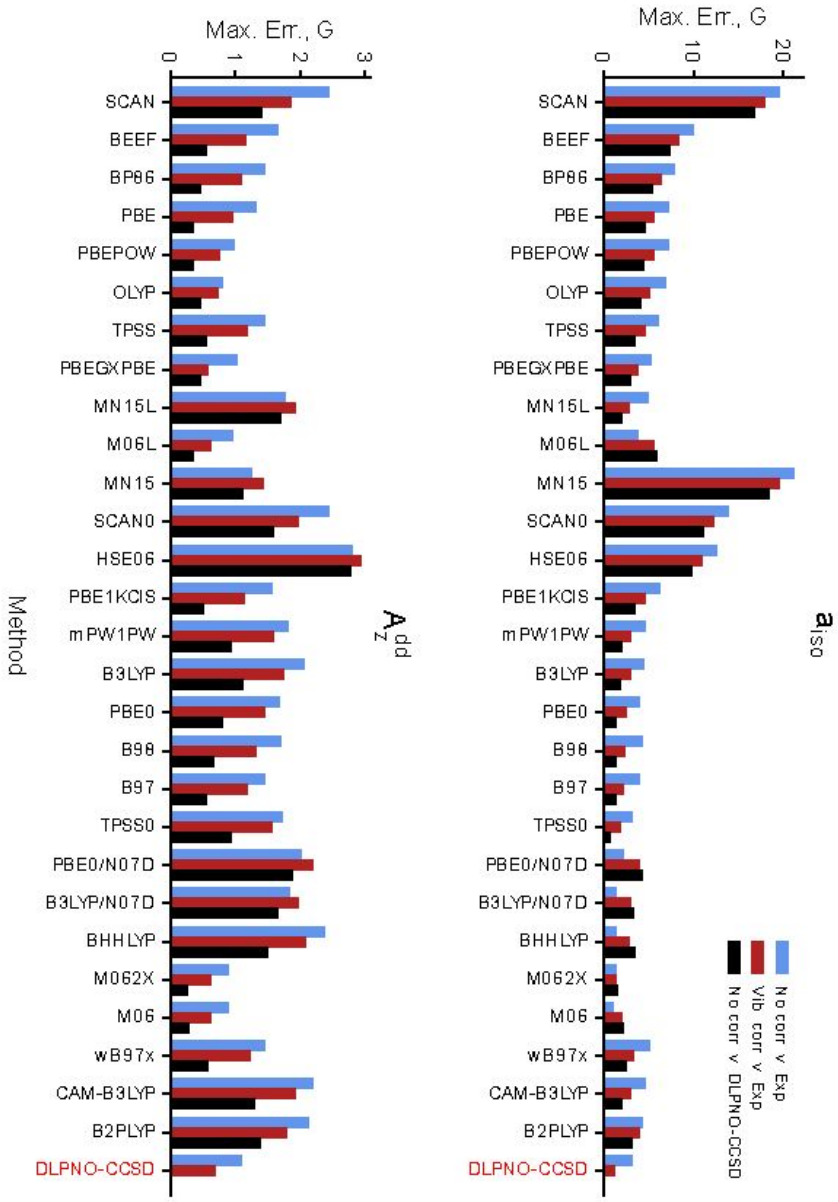


## Figure 3

Due to technical limitations, the caption for Figure 3 is only available in the manuscript.

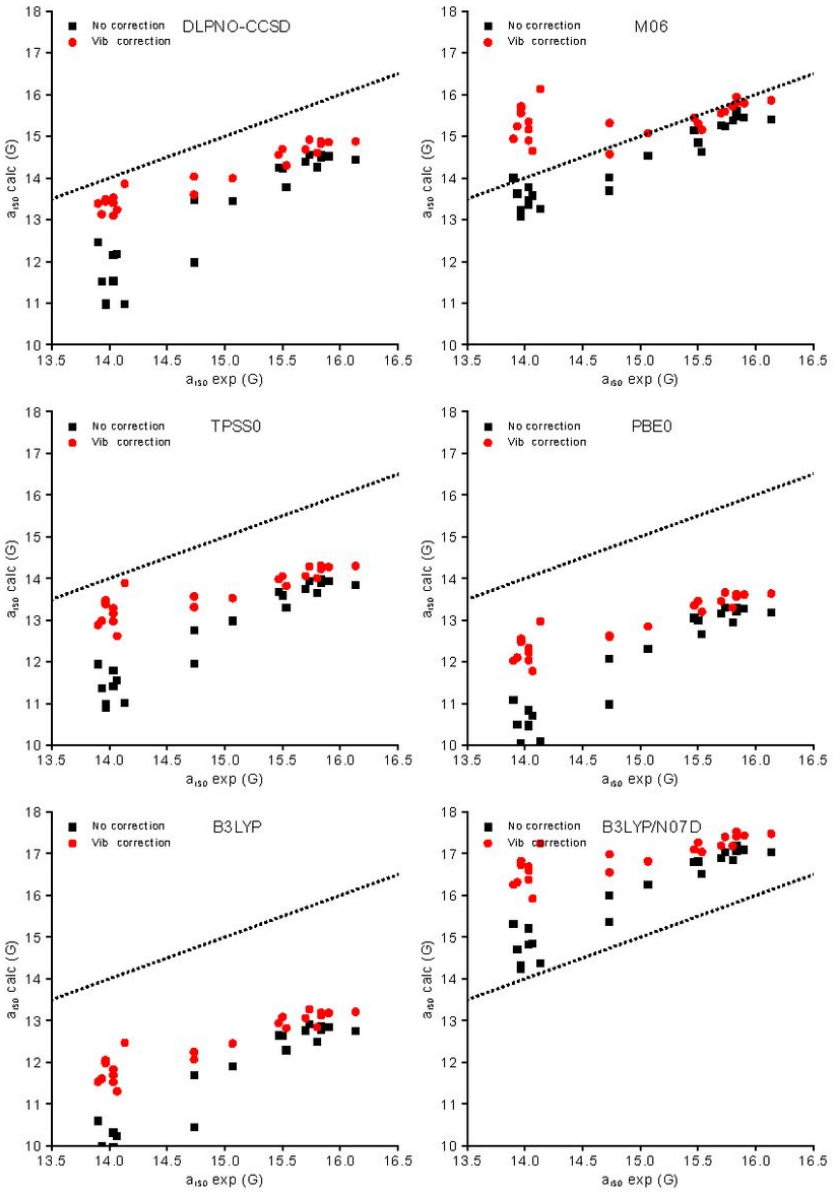


Figure 4

Plot of theoretical vs. experimental 14N aiso of the set of the nitroxide radicals used in the present study: without vibrational correction applied (black) and with the vibrational correction (red)

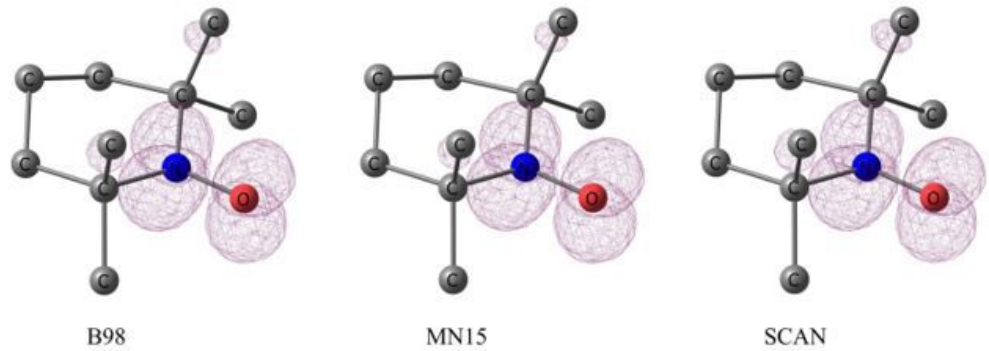


Figure 5

Spin density in radical VII (TEMPO) calculated at the UKS/B98/cc-pCVQZ-Juc, UKS/MN15/cc-pCVQZ-Juc, and UKS/SCAN0/ cc-pCVQZ-Juc levels. Contour value 0.0045.

## Supplementary Files

This is a list of supplementary files associated with this preprint. Click to download.

- gromovsupplementary.csv